U.S. DEPARTMENT OF COMMERCE
U.S. Environmental Science Services Administration
Weather Bureau

ESSA Technical Memorandum WBTM NMC 45

ON A CERTAIN TYPE OF INTEGRATION ERROR IN NUMERICAL WEATHER PREDICTION MODELS

Hans Økland

RAREBOOK
QC
996
.T33
no. 45

NATIONAL METEOROLOGICAL CENTER

SUITLAND, MD.
September 1969

National Oceanic and Atmospheric Administration

U.S. Joint Numerical Weather Prediction Unit

ERRATA NOTICE

One or more conditions of the original document may affect the quality of the image, such as:

Discolored pages
Faded or light ink
Binding intrudes into the text

This has been a co-operative project between the NOAA Central Library, National Center for Environmental Prediction and the U.S. Air Force. This project includes the imaging of the full text of each document. To view the original documents, please contact the NOAA Central Library in Silver Spring, MD at (301) 713-2607 x124 or www.reference@nodc.noaa.gov.

LASON
Imaging Contractor
12200 Kiln Court
Beltsville, MD 20704-1387
April 13, 2004

UDC 551.509.313:519.28

551.5	Meteorology
.509.313	Numerical prediction
519	Statistics
.28	Quality control of integration errors

CONTENTS

	Page
ABSTRACT	iv
1. Introduction	1
2. Description of the errors	2
3. Discussion of what causes the errors	5
4. Harmonic analysis of a specific case	8
5. Conclusions	15
ACKNOWLEDGMENTS	16
REFERENCES	17

ABSTRACT

Certain truncation errors occur in numerical weather prediction models when a grid-point representation of the variables is used to simulate advection phenomena. The errors are manifest by excessive values of the variables and by upstream propagation of small-scale noise. The mechanism causing these errors is studied by numerical experiments and harmonic analysis. Several ways to avoid or prevent errors of this kind are cited. Inclusion of a horizontal diffusion term in the scheme may be necessary to remove the errors completely.

ON A CERTAIN TYPE OF INTEGRATION ERROR IN NUMERICAL WEATHER PREDICTION MODELS

1. Introduction

Since primitive equation models came into use, much emphasis has been placed on the development of stable numerical schemes, and for good reason too, since a less stable scheme may not give a solution at all, or a very poor one. However, a stable scheme may also give a poor solution if it has large truncation errors (meaning errors made by using a grid representation of the variables, or a truncated series if the spectral method is used). True, the results computed by a stable scheme supposedly will converge to the exact solution for decreasing values of the time and space increments. However, the question of computer economy is always involved in operational predictions, and for that reason one does not want to decrease the grid increments more than absolutely necessary, and, if possible, improve the accuracy by some other means.

This paper is not intended to be a comprehensive study of these problems. Instead, we shall study a special type of error, which we believe is rather common when a grid-point representation is used. We shall try to determine the mechanism by which these errors develop, and also indicate one possible way to get rid of them.

A similar type of error was studied by Miyakoda (1960) from a more general point of view, and some of his results are analogous to the results we shall present in this paper.

2. Description of the errors

In a numerical experiment described by the author in another paper (Økland, 1969) a certain type truncation error was observed. The experiment was designed to simulate the development of a cyclone in a baroclinic flow, and a 4-level primitive equation model was used. The dependent variables were carried in the following levels: the earth's surface, the 700-mb pressure surface, the tropopause and the 50-mb pressure surface. Potential temperature, θ, was one of these variables, and in the lowest level prognostic values of θ were computed from the equation

$$\frac{\partial \theta}{\partial t} = -u\frac{\partial \theta}{\partial x} - v\frac{\partial \theta}{\partial y}, \tag{1}$$

where u and v are the horizontal velocity components. The finite difference scheme was of the "staggered" type described by Eliassen (1956).

In the experiment a cyclone gradually developed from an initially small disturbance, and after 3 days the surface potential temperature was as shown in Fig. 1. Warm air had moved to the north in front of the low, and cold air had moved southward behind it. Two areas with strong horizontal temperature gradients developed in front of the warm and cold tongues. They were associated with pressure troughs and wind shift, and therefore appeared to have the characteristic features of atmospheric fronts. It was shown that these fronts were created primarily by belt-shaped areas of strong convergence located along the thermal zone, and since the development of such areas of convergence was predictable from quasi-geostrophic theory, it was concluded that the experiment was

simulating a process which could take place in the real atmosphere.

In this lowest level the potential temperature initially was between 280°K and 300°K. Since θ, according to equation (1), is individually conserved, there should be no value outside this range at any later time. This was not the case, however. On the warmer side of the warm front the potential temperature had risen to more than 303°, and behind the cold front there were grid-point values about 2° below 280°. It was therefore obvious that the temperature field was also influenced by truncation errors which created excessive values on both sides of the fronts, and that these errors could distort the gradients created by the deformation in the wind field.

As the integration proceeded from three days to five days, these errors became larger, and they also showed a tendency to a wave-like propagation away from the front.

In order to study these integration errors more closely, some numerical experiments have been made, using different types of finite difference schemes for the integration of equation (1). Contrary to the case referred to above, the wind field was stationary in these experiments, since it was assumed that the time variation of the velocity was of minor importance compared to the space variation.

Figs. 2 to 5 show one such experiment. In Fig. 2 a part of the grid is shown. The initial grid values of θ were computed from

$$\theta_{i,j} = -10 \sin\left(\frac{\pi}{12} j\right).$$

Heavy lines are drawn for every 5 units in θ. Velocity components were derived from the formulas:

$$u_{i,j} = -0.3 \sin\left(\frac{\pi}{8} i - \frac{\pi}{12} j\right) \cdot (\Delta x) \cdot (\Delta t)^{-1}$$

$$v_{i,j} = 0.2 \sin\left(\frac{\pi}{8} i - \frac{\pi}{12} j\right) \cdot (\Delta x) \cdot (\Delta t)^{-1}.$$

Both velocity components are zero along the broken lines. The velocity is also indicated by arrows on Fig. 2, and the broken lines are seen to be lines of maximum convergence and divergence. A simple centered space and time difference scheme was used for the integration, and cyclic boundary conditions were applied both in x and in y direction. θ, u and v were given in all the grid-points (no staggered grid).

As shown in Fig. 3 and 4 large truncation errors developed, and they were of the type described earlier. A reduction of the length of the time-step by a factor of 10 caused only small changes in the results.

Fig. 5 shows the effect of adding a diffusion term of the usual Fickian type to the right hand side of (1). The exact solution (for the case without diffusion) may easily be derived. Compared to this solution the gradients in Fig. 5 are too weak, as might be expected.

It should perhaps be stressed that the diffusion is introduced for the only reason of controlling the truncation errors, and is not intended to simulate any physical effect. Also, there may be other and better ways of removing the errors, for instance, a space smoother applied periodically.

The diffusion coefficient, $5 \times 10^{-3} (\Delta x)^2 (\Delta t)^{-1}$, was determined by experiments. The optimum value obviously depends on the deformation of

the wind field. However, the wind field was chosen initially and kept unchanged in the experiment, while in general it is developed by the model itself. Therefore, the optimum value of the diffusion coefficient probably must be determined for each model, and should not be derived from the value given above.

3. Discussion of what causes the errors

Since the errors seem to be connected with the development of strong gradients in the dependent variable, there is reason to believe that they occur because the grid is unable to describe these strong gradients properly. In terms of energy spectrum considerations, one may say that there is a transfer of energy towards smaller scales because of the non-linear character of the governing differential equations. In case of a grid-point representation, a smallest scale exists, below which the grid is unable to represent the components properly (the "two grid-increment wave"). Because of the phenomenon generally called "aliasing", the still smaller scales may falsely be interpreted by the grid as components larger than two grid-increments (See Phillips 1959).

The diffusion, which proved to be an effective cure, removes energy from the small-scale part of the spectrum. The effect of this is partly to reduce the aliasing, since the diffusion tends to smooth the strong gradients, and partly to damp the false components which are produced by the aliasing, since these components also are mostly of short wave-lengths (see Section 4).

The errors demonstrated in the experiments showed two characteristic features. The one was the excessive values of the variable on both sides of the strong gradient. The other was the upstream propagation of small-scale errors. The latter feature may also be observed in connection with still simpler equations, like

$$\frac{\partial \theta}{\partial t} + U \frac{\partial \theta}{\partial x} = 0, \tag{2}$$

where U is a constant. Fig. 6 shows the initial values and the result of a numerical experiment based on equation (2), using a simple finite difference scheme, centered in space and time. The initial value of θ is 0 to the left of some specific grid point, but has a certain constant value in this point and all the other points to the right. The result after 50 time-steps shows that the "discontinuity" has become somewhat smoothed, but more interesting is the small-scale "noise" which is very noticeable upstream, but not downstream.

It is interesting to discuss this last observation in view of the group velocity concept. In contrast to the differential equation (2), the analogous difference equation has a dispersive character, since the phase velocity is a function of the wave length:

$$c = \frac{L}{2\pi \Delta t} \arcsin\left(\frac{U \Delta t}{\Delta x} \sin\left(\frac{2\pi \Delta x}{L}\right)\right)$$

where L is the wave length, Δx is the space increment, and Δt is the length of the time-step (Økland, 1958). From this relation one can easily compute the group velocity by means of the formula

$$c_g = c - L\frac{dc}{dL}.$$

(See for instance Lamb 1945). It turns out that the group velocity is 0 for $L = 4\Delta x$, and that it approaches U for large L. However, for wave lengths shorter than $4\Delta x$, the group velocity is negative, and it approaches - U when L approaches $2\Delta x$.

In order to understand how this can be applied to the experiment, it is necessary to bear in mind two facts. Firstly, the specified initial data give rise to energy on all wave-lengths larger than $2\Delta x$. Secondly, the energy in the different parts of the spectrum propagates with the group velocity rather than the phase velocity.

~~Looking~~ at Fig. 6, it is clear that the smallest scales are found farthest upstream, while scales which are a little longer also are found upstream, but not as far. Downstream, where the energy associated with the larger scales has propagated, the result is much more smooth. We may add a remark about the frequency. Since, according to the formula above, the phase velocity approaches 0 when L approaches $2\Delta x$, the local frequency of oscillation is small for the shortest scales. This was also confirmed by the experiment.

In order to explain the mechanism by which the errors develop, we have so far only offered some general remarks concerning the change in scale and aliasing, and we have also discussed the upstream propagation of the errors in view of the group velocity concept.

However, we have not offered any kind of proof that these effects really can produce the errors described. In an attempt to do so, we shall resort to harmonic analysis, taking into account the effect of aliasing in a similar manner as Phillips (1959). However, we shall restrict the analyses to the special case of solving a finite difference analogy to equation (2) where U now is a simple harmonic function of x.

4. Harmonic analysis of a specific case

Let us then assume that

$$U_j = \hat{U} \sin(2kj)$$

where $k = \frac{\pi}{N+1}$ and j may have integer values from 0 to N + 1 (Fig. 7). The dependent variable, θ, will be expressed by the series

$$\theta_j = a_0 + \sum_{n=1}^{N+1} a_n \cos(knj) \tag{3}$$

where the coefficients a_0 and a_n are functions of time.

Approximating the space derivative in (2) by centered differences, the second term of (2) may be written

$$U_j \frac{\theta_{j+1} - \theta_{j-1}}{2\Delta x} = \sum_{n=1}^{N+1} \frac{\hat{U} a_n \sin(2kj)}{2\Delta x} \left[\cos(kn(j+1)) - \cos(kn(j-1))\right]$$

$$= -\sum_{n=1}^{N+1} \frac{\hat{U} a_n \sin(kn)}{\Delta x} \left[\sin(2kj) \sin(knj)\right]$$

$$= \sum_{n=2}^{N-1} \frac{\hat{U} a_n \sin(kn)}{2\Delta x} \left[\cos(k(n+2)j) - \cos(k(n-2)j)\right]$$

$$+ \frac{\hat{U} a_1 \sin k}{2\Delta x} \left[\cos(3kj) - \cos(kj)\right] +$$

$$+ \frac{\hat{U} a_N \sin(kN)}{2\Delta x} \left[\cos(kNj) - \cos(k(N-2)j) \right]$$

We have here taken into account the fact that cos (k (N+2)j) = cos (kNj) for integer values of j, which demonstrates that k(N+1) = π corresponds to the so-called "folding frequency" in the theory of aliasing.

If now we write the first term in (2) as

$$\frac{da_0}{dt} + \sum_{m=1}^{N} \frac{da_m}{dt} \cos(kmj),$$

and collect terms belonging to the same Fourier component, we get a set of ordinary differential equations which must be satisfied if (3) shall be a solution of (2):

(4)

$$\frac{da_0}{dt} - K_2 a_2 = 0$$

$$\frac{da_1}{dt} - K_1 a_1 - K_3 a_3 = 0$$

$$\frac{da_2}{dt} - K_4 a_4 = 0$$

$$\frac{da_3}{dt} + K_1 a_1 - K_5 a_5 = 0$$

$$\frac{da_4}{dt} + K_2 a_2 - K_6 a_6 = 0$$

. . . . . .

$$\frac{da_{N-2}}{dt} + K_{N-4} a_{N-4} - K_N a_N = 0$$

$$\frac{da_{N-1}}{dt} + K_{N-3} a_{N-3} = 0$$

$$\frac{da_N}{dt} + K_N a_N + K_{N-2} a_{N-2} = 0$$

$$\frac{da_{N+1}}{dt} + K_{N-1} a_{N-1} = 0$$

where

$$K_n = \frac{\hat{U} \sin(kn)}{2\Delta x}$$

Inspecting the equations (4) we note that the first and the last equations are the only ones which contain a_0 and a_{N+1}, respectively. Therefore, the system may be solved without these equations, and a_0 and a_{N+1} can be derived afterwards. Multiplying the remaining N equations by K_1a_1, K_2a_2, ... , K_Na_N, respectively, and adding them together, one gets

$$\frac{1}{2}\frac{d}{dt}\left(K_1a_1^2+\dots+K_Na_N^2\right)=K_1^2a_1^2-K_N^2a_N^2. \tag{5}$$

We also note that the equations (4) contain terms with either even or odd indices, which shows that (4) may be split into two systems, one of which contains only terms with odd indices. From this sub-system one may derive an equation similar to (5), which also contains only "odd" terms, and we note that this equation will not contain a_N if N is even, and therefore must be of the form

$$\frac{1}{2}\frac{d}{dt}\left(K_1a_1^2+K_3a_3^2+\dots\right)=K_1^2a_1^2. \tag{6}$$

Therefore, if the quantity on the left hand side of (5) shall stay less than a certain number for any value of t, one must have $a_1 = 0$ from a certain time, t_1 say. However, the second equation (4) shows that this can only be the case if a_3 stays equal to zero. Proceeding in the same manner, one concludes that from time t_1 all the a's with odd numbers must be zero. But this can only be the case if they all are zero initially, which is easily concluded from (6). This, by the way, is the condition for the initial values being symmetric with respect to the point where U = 0.

We shall now work out the complete solution for one actual case. We shall choose an odd value of N. The considerations above, which led to a conclusion we might call a sufficient condition for instability, does not apply to this case, and it may be of interest to see what type of solution we then can have. We also want to keep the order of the system (4) so low that the solution can be found without resorting to complicated numerical methods. A non-trivial case turns out to be N = 5 (Fig. 7).

Introducing

$$a_n = \hat{a}_n e^{ict}, \; n = 1, 2, .. 5 ,$$

and taking into account the fact already mentioned that the system (4) splits into an even and an odd part, we get the following two sets of linear homogeneous equations

$$ic\hat{a}_0 - K_2\hat{a}_2 = 0$$

$$ic\hat{a}_2 - K_4\hat{a}_4 = 0$$

$$ic\hat{a}_4 + K_2\hat{a}_2 = 0$$

$$ic\hat{a}_6 + K_4\hat{a}_4 = 0$$

and

$$ic\hat{a}_1 - K_1\hat{a}_1 - K_3a_3 = 0$$

$$ic\hat{a}_3 + K_1\hat{a}_1 - K_5a_5 = 0$$

$$ic\hat{a}_5 + K_5\hat{a}_5 + K_3\hat{a}_3 = 0.$$

The characteristic equations for these two systems are

$$c^2 (c^2 - K_2{}^2) = 0$$

and

$$c\,(c^2 - 2K_1 K_3 + K_1^2) = 0$$

respectively, when we take into account that $K_1 = K_5$ and $K_2 = K_4$. Since all the roots of this equation turn out to be real, we obviously have a stable solution. Let us further state the initial values as $\theta_j = \cos(kj)$, which means that $a_1 = 1$ and $a_n = 0$ for $n > 1$. One realizes immediately that $a_0 = a_2 = a_4 = a_6 = 0$ at any later time. The solution for a_1, a_3 and a_5 may easily be worked out, following the standard methods. We skip the rather lengthy calculations and give the final solution:

$$a_1 = \frac{K_1 K_3 - K_1^2}{c_1^2} \cos(c_1 t) + \frac{K_1}{c_1} \sin(c_1 t) + \frac{K_1 K_3}{c_1^2}$$

$$a_3 = \frac{K_1^2}{c_1^2} \cos(c_1 t) - \frac{K_1}{c_1} \sin(c_1 t) - \frac{K_1^2}{c_1^2}$$

$$a_5 = -\frac{K_1 K_3}{c_1^2} \cos(c_1 t) + \frac{K_1 K_3}{c_1^2}$$

where c_1 is the positive root of

$$c_1^2 = 2K_1 K_3 - K_1^2.$$

Inserting this in (3) and introducing the actual values of K_1 and K_3 we finally get:

$$\theta_0 = 1$$

$$\theta_1 = \cos\left(c_1 t - \frac{\pi}{6}\right)$$

$$\theta_2 = \sin\left(c_1 t - \frac{\pi}{6}\right) + 1$$

$$\theta_3 = 0$$

$$\theta_{3+j} = -\theta_{3-j}; \; j = 1, 2, 3$$

From this solution it may for instance be seen that θ_2 increases from its initial value until it reaches the value 2 when $c_1 t = 2\pi/3$. At that time θ_1 has decreased to 0 after first having increased to the value 1. This is essentially the same behavior as in the experiments described earlier.

So far we have made no assumptions concerning the finite difference approximation in time. The results we have derived may in general be considered to be valid for a very small centered time-step of length Δt, since the truncation errors connected with such a time-step is of second order with respect to Δt, while the number of time-steps needed depend linearly on Δt.

In the case for which we have worked out the final solution, it is easy to give the solution also for a centered finite time-step, defined by

$$\frac{da_n}{dt} = \frac{a_n^{(\tau+1)} - a_n^{(\tau-1)}}{2\Delta t}.$$

Assuming

$$a_n^{(\tau)} = \tilde{a}_n e^{i\nu\tau}$$

where τ is the number of steps, we get

$$\nu = \arcsin(c_1 \Delta t),$$

where ν is assumed less than $\pi/2$, and it is seen that we get basically the same type of solution as before if $/c_1 \Delta t/ < 1$, which means that the usual linear stability criterion has to be satisfied. We have then disregarded the fact that there also exists a so-called computational mode, corresponding to

$$\nu' = \pi - \nu.$$

This value does not converge towards $c_1 \Delta t$ for decreasing Δt, and must be considered as a false solution. It can usually be kept small in actual computations, as has been discussed elsewhere (Økland, 1958).

5. Conclusions

In this paper we have described a certain pattern of numerical errors which occur when strong gradients are formed during the time integration. It has been shown that the errors are tied to the representation of data by grid values, and an attempt has been made to uncover the mechanism by which they form. Of course, the question arises about the extent to which strong gradients develop in numerical weather prediction models. Classically they may develop because of the deformation properties of the non-divergent wind, but it is the belief of this author that strong irrotational wind fields in primitive equation models, and especially in the boundary layer, is much more important. Further, if the model has energy sources and sinks tied to the geography (mountains, coastlines, etc.), this could also develop strong gradients in the dependent variables.

One obvious way to avoid errors of this kind would be to have more grid points where the gradients become stronger. A grid based on a Lagrangian description could probably be designed so that it has this property. Another way would be to prevent the gradients from becoming too strong. This may be done by means of a horizontal diffusion term as shown in this paper. Some finite difference schemes have a built-in smoothing effect on the smallest scales. One of the experiments described earlier in this paper (Figs. 2, 3, 4 and 5) has been repeated using the scheme described by Shuman and Hovermale (1968), and the errors turned out to be smaller. However, in order to remove them completely it was necessary to include a diffusion term also in this scheme.

ACKNOWLEDGMENTS

The author is indebted to Dr. John A. Brown, Jr. for valuable discussions, and to Mrs. Zelda Licausi for typing the manuscript.

REFERENCES

Eliassen, A., "A Procedure for Numerical Integration of the Primitive Equations of the Two-Parameter Model of the Atmosphere," Scientific Report No. 4, on Contract AF19(604)-1286 University of California at Los Angeles, Dept. of Met., March 1956, 53 pp.

Kurihara, Y., "On the Use of Implicit and Iterative Methods for the Time Integration of the Wave Equation" Monthly Weather Review, Vol. 93, No. 1, January 1965, pp. 33-46.

Lamb, H., "Hydrodynamics," Dover Publications, New York, 1945, p.381.

Miyakoda, K., "The Methods of Numerical Integration of One-Dimensional Linear Equations and Their Inherited Errors," Journal of the Meteorological Society of Japan, Vol. 38, No. 6, 1960, pp. 259-286.

Økland, H., "Experimental Integration of a Four-Level Primitive Equation Model," Tellus, 21, 3, 1969, pp. 359-366.

Økland, H., "False Dispersion as a Source of Integration Errors," Scientific Reports No. 1, Norske Meteorologiske Institutt, Oslo, 1958.

Phillips, N. A., "An Example of Non-Linear Computational Instability," The Atmosphere and the Sea in Motion, Rockefeller Institute Press, New York, 1959, pp. 501-504.

Shuman, F. G., and Hovermale, J. B., "An Operational Six-Layer Primitive Equation Model," Journal of Applied Meteorology, Vol. 7, No. 4, August 1968, pp. 525-547.

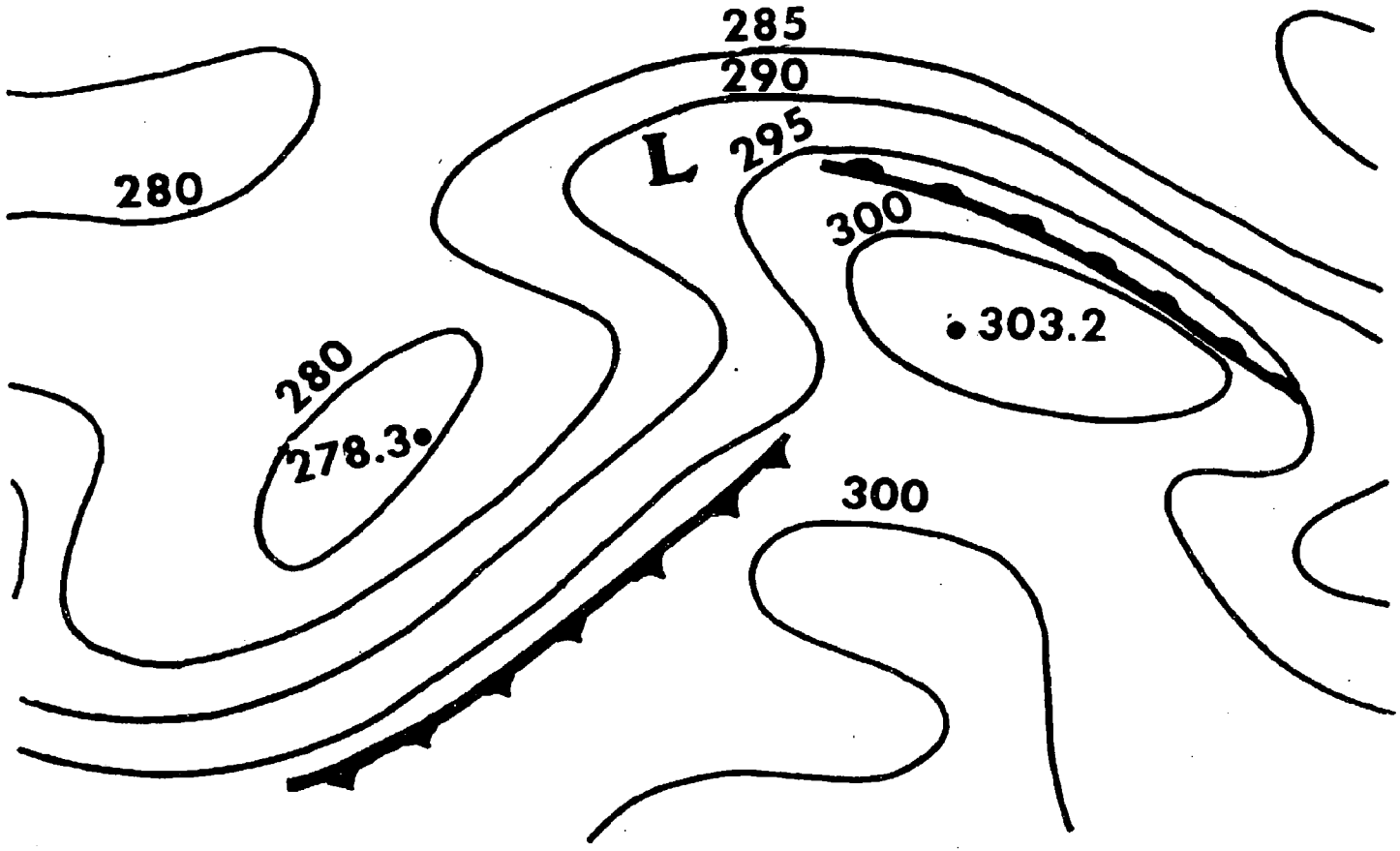

Figure 1.--Surface low, potential temperature, and two fronts from an experiment with a 4-level model which developed a cyclone and two fronts after three days, starting with baroclinic flow and a small perturbation.

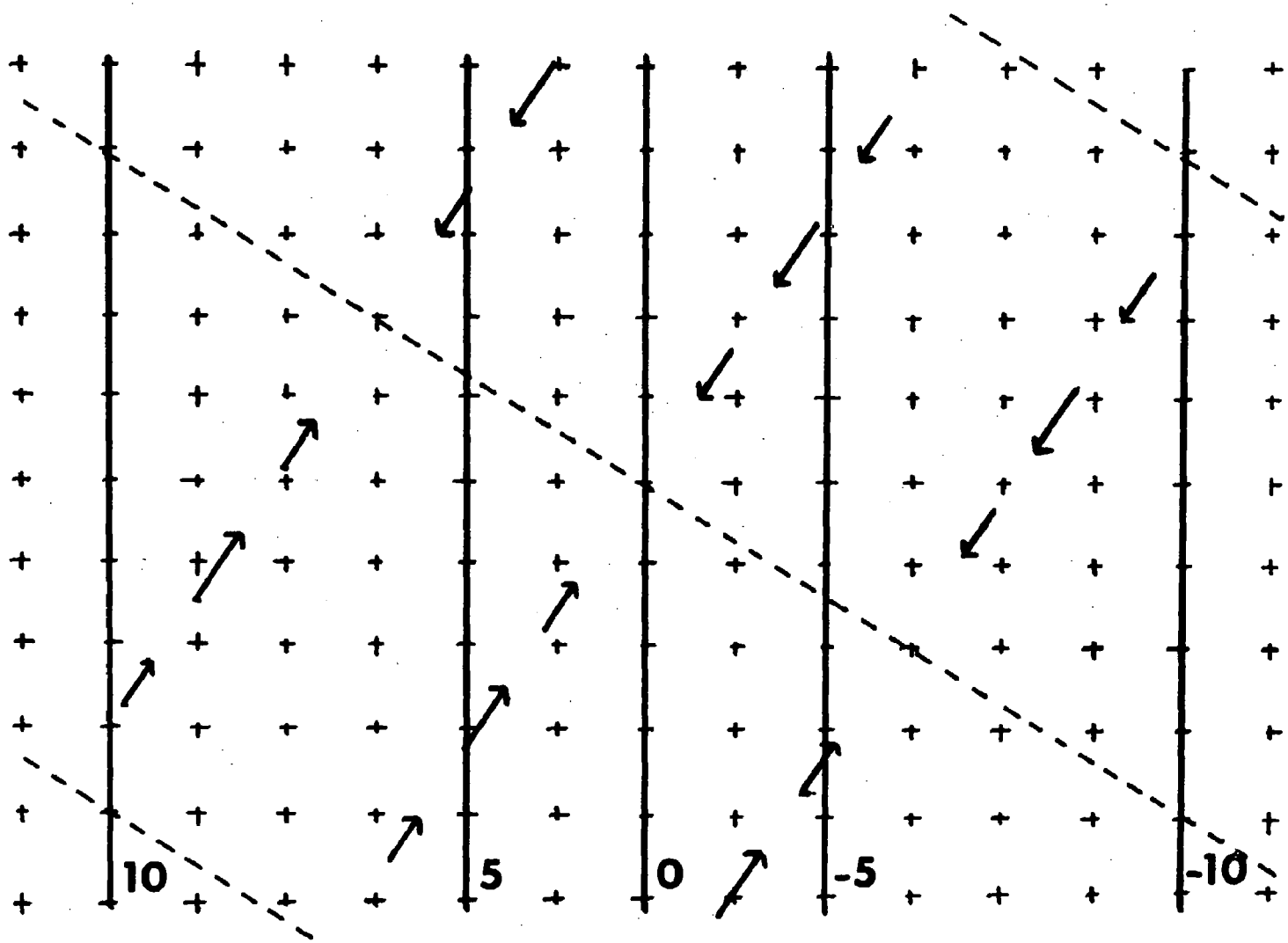

Figure 2.--Location of grid points and initial values for experimental integration of simple advection equation (1). Lines for dependent variable are drawn at intervals of five units; wind field is indicated by arrows; broken lines are maximum and minimum horizontal divergence.

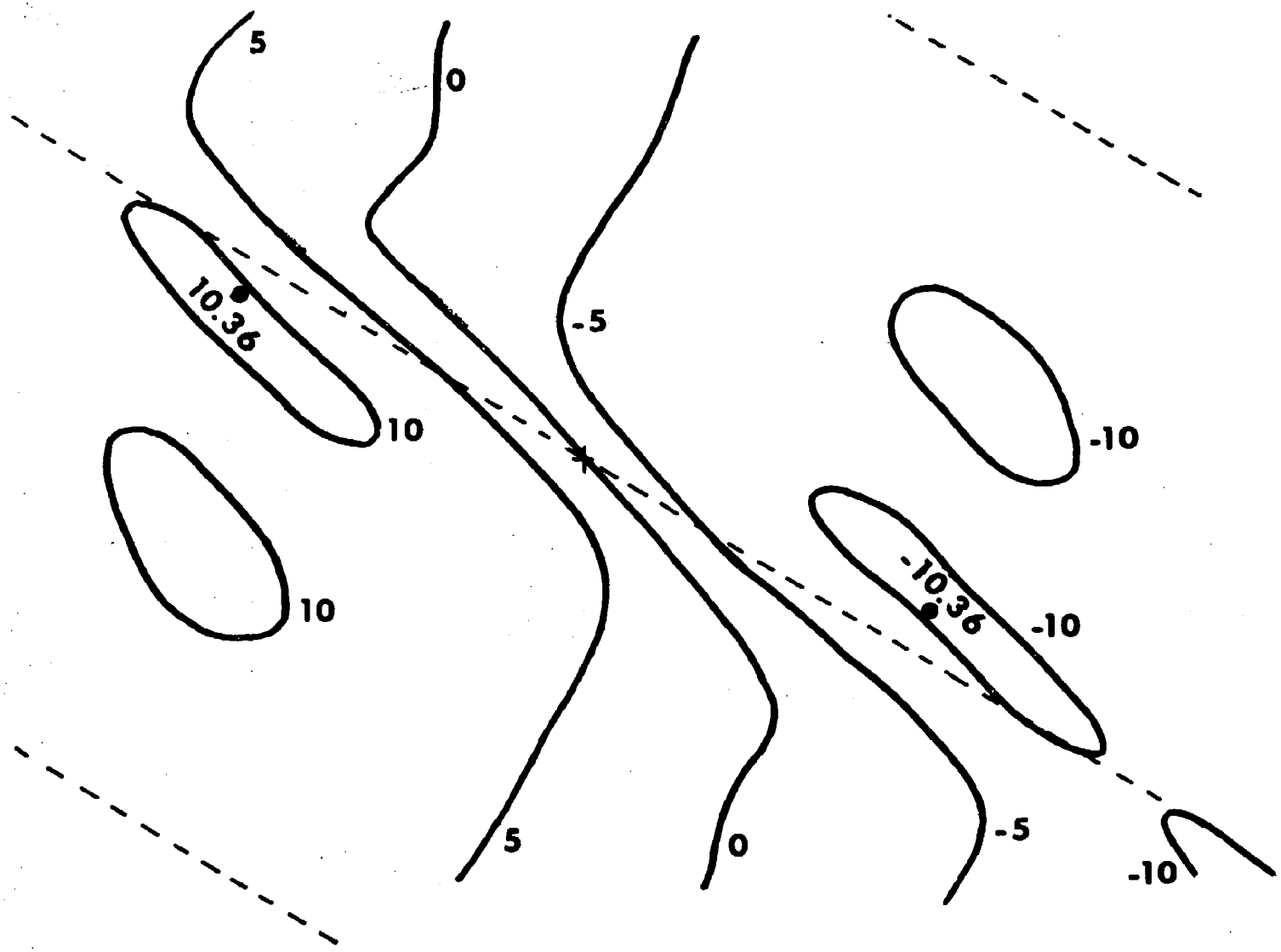

Figure 3.--Result after integrating equation (1) for five time-steps, starting with the values in figure 2.

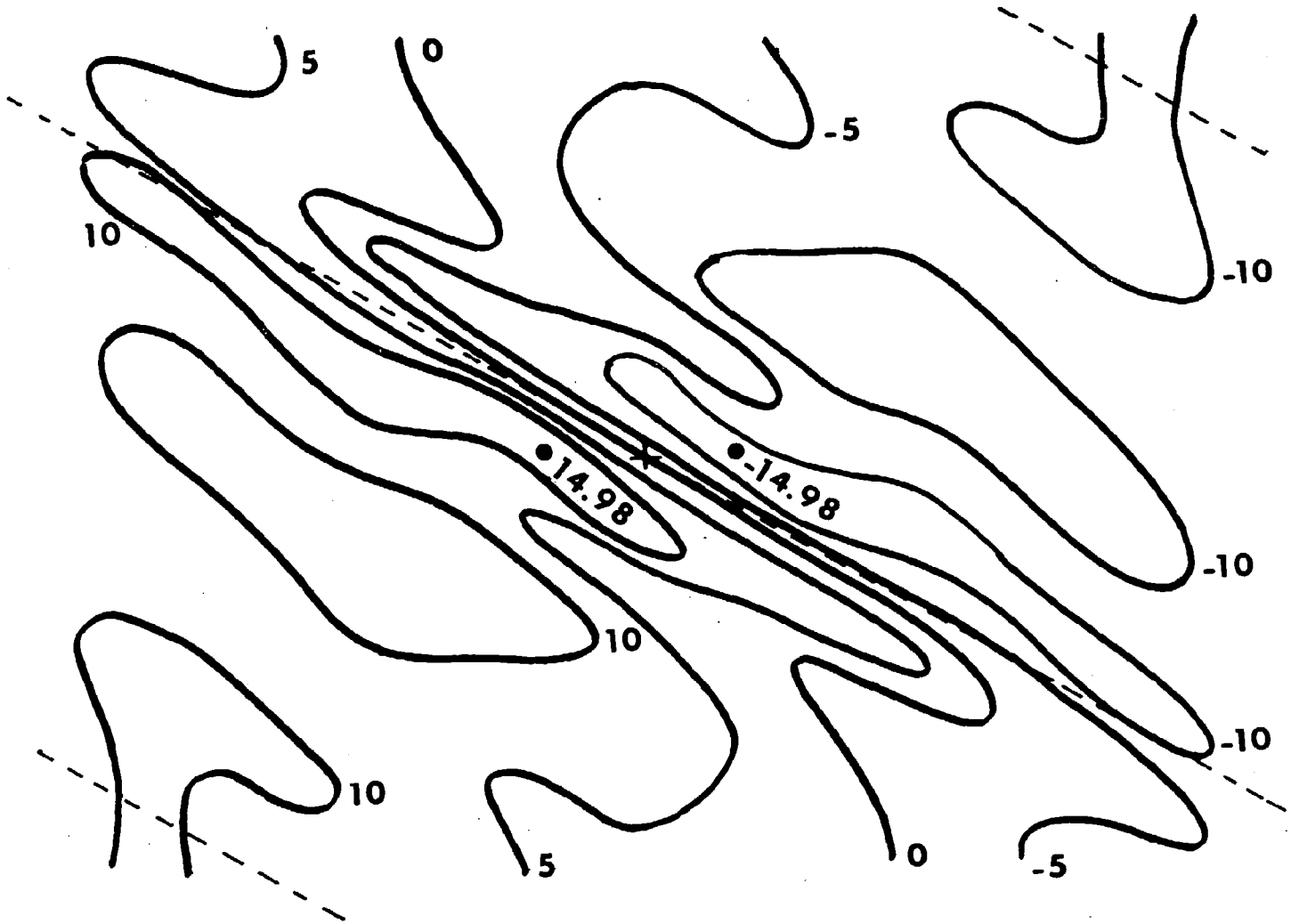

Figure 4.--Result after ten time-steps of the same integration as in figure 3.

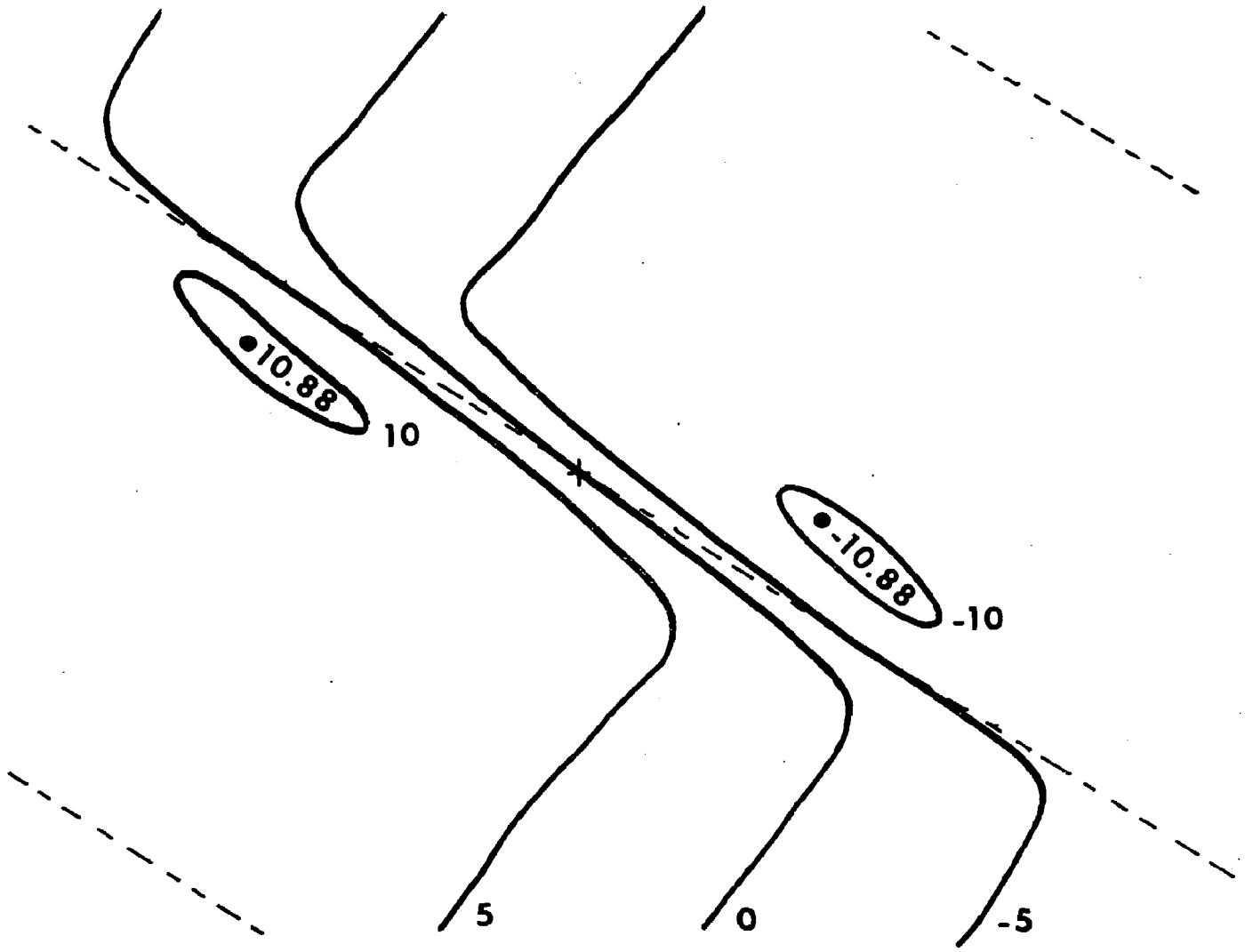

Figure 5.--Result after including a diffusion term in equation (1). In all other respects these results correspond to those demonstrated in figure 4.

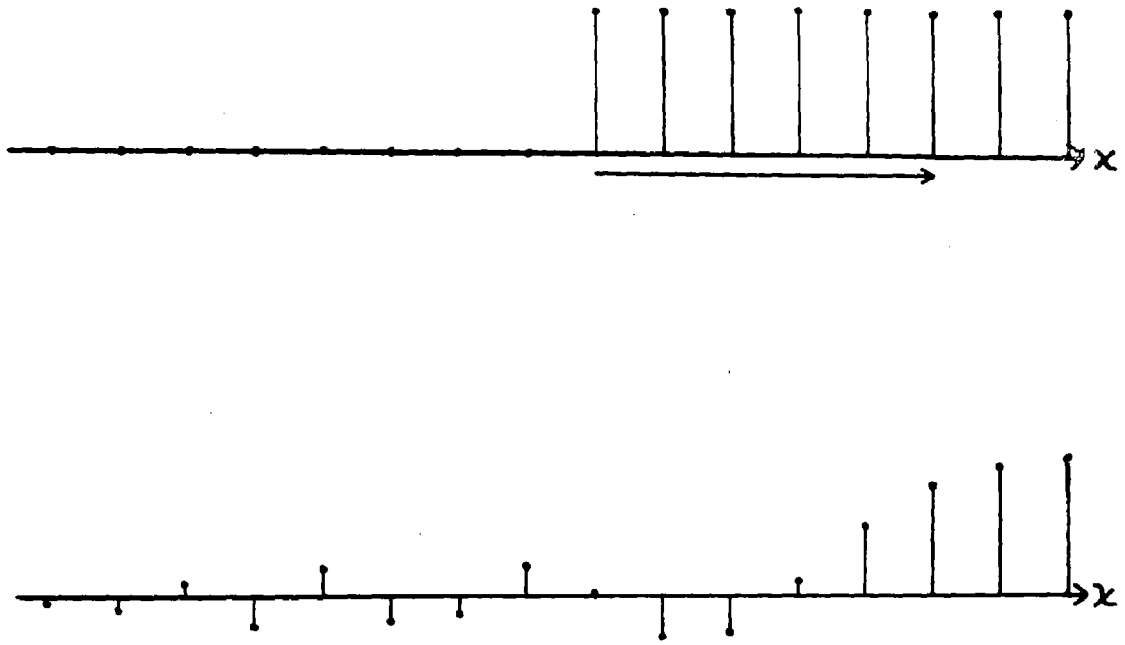

Figure 6.--Initial grid-point values (above) and result (after 50 time-steps) of one experiment with equation (2). Corresponding exact solution would have initial values displaced five increments to the right.

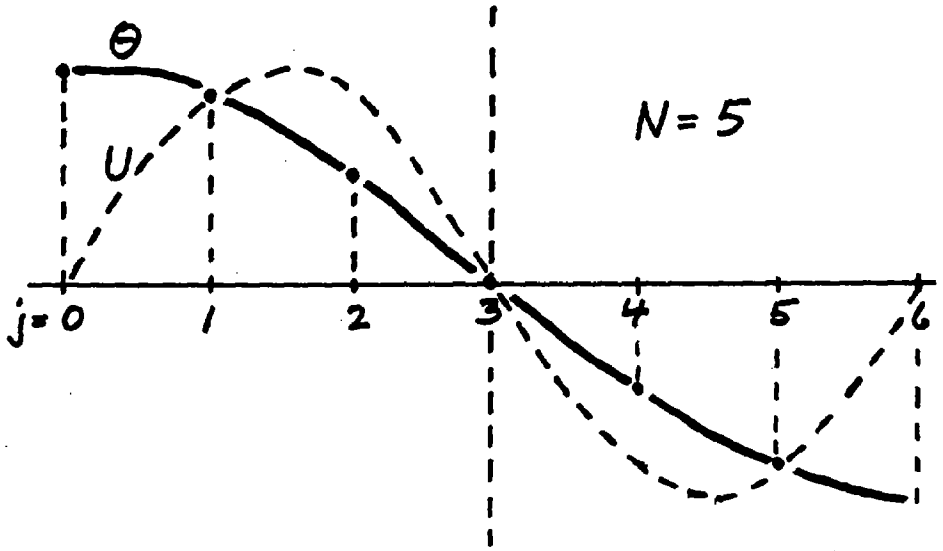

Figure 7.--This figure demonstrates assumptions underlying the harmonic analyses. The actual values given for N and θ are those for which the final solution is worked out.